Psychiatry Research: Neuroimaging 289 (2019) 26–36

Contents lists available at ScienceDirect

Psychiatry Research: Neuroimaging

journal homepage: www.elsevier.com/locate/psychresns

Alterations in white matter microstructure and cortical thickness in individuals at ultra-high risk of psychosis: A multimodal tractography and surface-based morphometry study

Alexander S. Tomyshev[a,*], Irina S. Lebedeva[a], Tolibdzhon A. Akhadov[b], Maria A. Omelchenko[c], Andrey O. Rumyantsev[c], Vasiliy G. Kaleda[c]

[a] Laboratory of Neuroimaging and Multimodal Analysis, Mental Health Research Center, 34 Kashirskoe shosse, 115522 Moscow, Russia
[b] Department of Radiology, Children's Clinical and Research Institute of Emergency Surgery and Trauma, Moscow, Russia
[c] Department of Endogenous Mental Disorders, Mental Health Research Center, Moscow, Russia

ARTICLE INFO

Keywords:
Ultra-high risk of psychosis
Tractography
Radial diffusivity
Surface-based morphometry
Cortical thickness
Frontal lobe
Parietal lobe

ABSTRACT

There is increasing evidence of white matter (WM) and grey matter pathology in subjects at ultra-high risk of psychosis (UHR), although a limited number of diffusion-weighted magnetic resonance imaging (DW-MRI) and surface-based morphometry (SBM) studies have revealed anatomically inconsistent results. The present multimodal study applies tractography and SBM to analyze WM microstructure, whole-brain cortical anatomy, and potential interconnections between WM and grey matter abnormalities in UHR subjects. Thirty young male UHR patients and 30 healthy controls underwent DW-MRI and T1-weighted MRI. Fractional anisotropy; mean, radial, and axial diffusivity in 18 WM tracts; and vertex-based cortical thickness, area, and volume were analyzed. We found increased radial diffusivity in the left anterior thalamic radiation and reduced bilateral thickness across the frontal, temporal, and parietal cortices. No correlations between WM and grey matter abnormalities were identified. These results provide further evidence that WM microstructure abnormalities and cortical anatomical changes occur in the UHR state. Disruption of structural connectivity in the prefrontal-subcortical circuitry, likely caused by myelin pathology, and cortical thickness reduction affecting the networks presumably involved in processing and coordination of external and internal information streams may underlie the widespread deficits in neurocognitive and social functioning that are consistently reported in UHR subjects.

1. Introduction

The concept of a clinical high-risk state of psychosis (CHR) has evolved to include the prepsychotic stage, which pertains to the individuals presenting with potential prodromal symptoms (Fusar-Poli et al., 2013). Two broad sets of criteria have been used to diagnose the CHR state: basic symptom criteria, identifying an earlier potentially prepsychotic stage, and ultra-high risk (UHR) criteria, reflecting a somewhat later phase (Fusar-Poli et al., 2013; Keshavan et al., 2011; Olsen and Rosenbaum, 2006). Hereinafter, we will use the term "UHR patients" to refer to the individuals who meet the UHR criteria (see Section 2.1. for the detailed UHR criteria used in the present study).

Studying UHR patients provides an opportunity to explore potential structural markers of the illness during a period characterized by significantly fewer confounds than full-blown psychosis. Such markers include diffusivity parameters of white matter (WM) fascicles and anatomical characteristics of the cerebral cortex, both of which were explored in the present study.

Diffusion-weighted magnetic resonance imaging (DW-MRI) has been increasingly applied in studies of schizophrenia patients. These studies have revealed widespread aberrations in WM microstructure in various regions, such as the corpus callosum; cingulum; uncinate fasciculus; inferior longitudinal fasciculus; superior longitudinal fasciculus; fronto-occipital fasciculus; and internal capsule, including the anterior and superior thalamic radiations (Parnanzone et al., 2017). However, relatively fewer studies have investigated WM structure in UHR patients (see Table 1 for an overview). Similar to the findings in schizophrenia patients, most of the studies have found that UHR patients exhibit widespread alterations in WM microstructure, mainly characterized by fractional anisotropy (FA) reduction (Bloemen et al., 2010; Cho et al., 2016; Karlsgodt et al., 2009; Katagiri et al., 2015; Krakauer et al., 2017, 2018; Peters et al., 2009; Rigucci et al., 2016;

* Corresponding author.
E-mail address: alexander.tomyshev@ncpz.ru (A.S. Tomyshev).

https://doi.org/10.1016/j.pscychresns.2019.05.002
Received 13 July 2018; Received in revised form 24 February 2019; Accepted 8 May 2019
Available online 09 May 2019
0925-4927/

Table 1
Overview of DW-MRI studies on UHR.

Author and year of publication	Methodology	Differences between UHR and HC	Differences between UHR-P and UHR-NP
Peters et al. (2008)	Tractography ROI	FA: negative	(Not tested)
Karlsgodt et al. (2009)	TBSS ROI	FA: UHR < HC, SLF (collapsed over two hemispheres)	(Not tested)
Peters et al. (2009)	VBA	FA: UHR < HC, r superior frontal lobe, l middle frontal lobe	(Not tested)
Bloemen et al. (2010)	VBA	FA: UHR-P < HC, l&r superior frontal lobe (ATR, IFOF)	FA: UHR-P < UHR-NP, lateral to r putamen (UNC, IFOF, SLF), l superior temporal lobe (SLF, IFOF, ILF); CHR-P > CHR-NP, l medial temporal lobe (PTR, IFOF, ILF)
Peters et al. (2010)	Tractography ROI	FA: negative	(Not tested)
Carletti et al. (2012)	VBA	FA, RD, AD: negative	FA, RD, AD: negative
von Hohenberg et al. (2014) [a]	TBSS whole brain	FA, AD: negative MD: CHR > HC, r (SLF, PCR, PLIC, SCR, cerebral peduncle, RLIC, cingulum (cingulate part), PTR, ALIC, fornix/stria terminalis, EC), splenium and body of CC RD: CHR > HC, r PRC	(Not tested)
Katagiri et al. (2015)	TBSS whole brain	FA: UHR < HC, genu and body of the CC	(Not tested)
Schmidt et al. (2015)	TBSS whole brain and ROI (SLF)	FA: UHR > HC, r ATR, IFOF, SLF, l UNC, r ILF, forceps major MD: UHR < HC, l ILF, l IFOF, SLF, r ILF	(Not tested)
Cho et al. (2016)	Tractography ROI	Relative connectivity: UHR < HC between thalamus and orbitofrontal cortex FA: UHR < HC between thalamus and orbitofrontal cortex	(Not tested)
Wang et al. (2016a)	TBSS whole brain	RD, MD: negative FA: UHR < HC, l (cingulum, CC, UNC, IFOF, SLF, ATR), forceps minor AD: UHR < HC, cingulum, CC	FA: UHR-P < UHR-NP, forceps minor
Rigucci et al. (2016)	TBSS whole brain	(Not tested)	FA: UHR-P < HC, l (SLF, corticospinal tract, ATR, IFOF, ILF), forceps major, body and splenium of the corpus callosum RD: UHR-P > HC, r corticospinal tract, forceps major, body and splenium of the corpus callosum
Krakauer et al. (2017)	TBSS whole brain	AD, RD: negative FA: UHR < HC, l SLF, r IFOF, l ATR	(Not tested)
Saito et al. (2017)	Tractography ROI	FA: UHR < HC, entire, genu, trunk, and splenium of the corpus callosum	FA: UHR-P > UHR-NP, genu and trunk of the corpus callosum
Krakauer et al. (2018)	TBSS whole brain	FA: UHR < HC, l corticospinal tract, r ATR, l SLF	(Not tested)

FA, fractional anisotropy; MD, mean diffusivity; RD, radial diffusivity; AD, axial diffusivity; UHR, ultra high risk; NC, normal controls; UHR-P, UHR individuals later converting to psychosis; UHR-NP, UHR individuals who did not later convert psychosis; CHR, clinical high risk; VBA, voxel-wise whole-brain analysis; TBSS, tract-based spatial statistics (Smith et al., 2006); ROI, region of interest; r, right; l, left; SLF, superior longitudinal fasciculus; ATR, anterior thalamic radiation; UNC, uncinate fasciculus; IFOF, inferior fronto-occipital fasciculus; ILF, inferior longitudinal fasciculus; PTR, posterior thalamic radiation; EC, external capsule; IC, internal capsule; PLIC, posterior limb of internal capsule; RLIC, retrolenticular part of internal capsule; ALIC, anterior limb of internal capsule; PCR, posterior corona radiata; SCR, superior corona radiata.

[a] The inclusion criteria in von Hohenberg et al. (2014) incorporated different approaches, including criteria of early and late prodromal phases.

Saito et al., 2017; Wang et al., 2016b), although a few studies found no aberrations, (Carletti et al., 2012; Peters et al., 2008, 2010; von Hohenberg et al., 2014) or even an increase (Schmidt et al., 2015), in the FA in UHR patients compared with healthy controls. Although the findings for some brain regions, such as the superior longitudinal fasciculus (Karlsgodt et al., 2009; Krakauer et al., 2017, 2018; Rigucci et al., 2016; von Hohenberg et al., 2014; Wang et al., 2016a) and anterior thalamic radiation (ATR) (Bloemen et al., 2010; Krakauer et al., 2017, 2018; Rigucci et al., 2016; Wang et al., 2016a), have been reproduced, the DW-MRI results obtained from UHR patients appear rather heterogeneous, perhaps due to diversity of methods, study populations, and employed diagnostic criteria. However, even the results of studies using similar processing methods, e.g., tract-based spatial statistics, are inconsistent (Katagiri et al., 2015; Krakauer et al., 2018; Rigucci et al., 2016; Schmidt et al., 2015; von Hohenberg et al., 2014; Wang et al., 2016a).

A number of studies have found grey matter volume deficits in UHR patients that are similar, although to a low extent, to the deficits observed in schizophrenia patients (Bartholomeusz et al., 2017; Brent et al., 2013; Fusar-Poli et al., 2011a). Surface-based morphometry (SBM) has been increasingly utilized in this context, and has provided additional information over that afforded by conventional volumetric analysis. While voxel-based morphometry only measures volume, SBM assesses volume and its separate components, cortical thickness and surface area, which are both highly heritable but influenced by different, uncorrelated genetic factors (Panizzon et al., 2009). However, with respect to the cortical anatomical alterations observed in UHR patients, SBM findings remain inconsistent, which may be caused by differences in the study populations and employed diagnostic criteria. Cortical thickness reduction in UHR patients has been shown to spread across the brain, including the temporal, cingulate, parahippocampal, prefrontal, parietal, and insular cortices (Benetti et al., 2013; Fornito et al., 2008; Gisselgard et al., 2018; Jung et al., 2011; Kwak et al., 2018; Takayanagi et al., 2017; Tognin et al., 2014), although 5 of the 12 published SBM studies have reported no cortical thickness differences between UHR and control groups (Bakker et al., 2016; Cannon et al., 2015; Haller et al., 2009; Klauser et al., 2015; Ziermans et al., 2012). Furthermore, a previous study has revealed bidirectional alterations in the UHR cohort compared with controls using voxel-based cortical thickness maps (Dukart et al., 2017). Three SBM studies have analyzed surface area along with cortical thickness (Bakker et al., 2016; Fornito et al., 2008), and only one of them has revealed, using an ROI-based approach, a larger area of the left anterior cingulate gyrus in the UHR patients compared with healthy controls (Takayanagi et al., 2017).

According to the mechanical models of brain development, cortical gyrification and variations in cortical thickness are considered to be influenced by the axonal tension exerted between linked areas (Hilgetag and Barbas, 2006; Van Essen, 1997). Therefore, the

development of WM connectivity and cortical thickness may be interconnected. Indeed, it has been shown that age-related changes in cortical grey matter and WM integrity are negatively correlated in healthy adolescents and young adults (Giorgio et al., 2008; Tamnes et al., 2010). Consequently, it is reasonable to hypothesize that WM microstructure and cortical thickness abnormalities develop in an intertwined manner in UHR patients. However, to the best of our knowledge, no study has combined structural MRI and DW-MRI to investigate the associations of WM and grey matter abnormalities in UHR patients. As structural neuroimaging findings in UHR patients resemble the patterns of WM and grey matter disruptions reported in schizophrenia, although less prominent (Bartholomeusz et al., 2017; Bois et al., 2015), we expected that a disturbed WM microstructure would be associated with decreased cortical thickness in the anatomically connected brain regions, similar to the disruptions observed in schizophrenia patients (Fusar-Poli et al., 2013; Keshavan et al., 2011; Olsen and Rosenbaum, 2006).

The aims of this multimodal exploratory study were: 1) to compare the diffusivity measures of WM tracts and the anatomy of cortical grey matter between a homogenous group of young male UHR patients and healthy controls, and 2) to examine the potential relationship between the changes in WM microstructure and cortical thickness in the UHR group.

To the best of our knowledge, the present study is the first to utilize global probabilistic tractography with prior information of tract anatomy (TRActs Constrained by UnderLying Anatomy, TRACULA) (Yendiki et al., 2011) in UHR patients. This method uses not only DW-MR images but also anatomical reconstructions derived from T1-weighted MR images. Further, unlike most of the previous studies (Bloemen et al., 2010; Cho et al., 2016; Karlsgodt et al., 2009; Krakauer et al., 2018; Peters et al., 2008, 2010, 2009; Saito et al., 2017; Schmidt et al., 2015), the present study analyzes radial diffusivity (RD) and axial diffusivity (AD) values in addition to aggregated measures of FA and mean diffusivity (MD). In addition to exploring differences in overall directionality or diffusivity, this analysis allowed us to propose hypotheses regarding the type of WM abnormalities that cause such differences. In particular, an increased RD is believed to characterize myelin pathology, while a decreased AD presumably indicates axonal damage (Aung et al., 2013). Moreover, two previous tractography studies of UHR patients analyzed only the four fiber tracts that have been shown to be affected in schizophrenia patients (Peters et al., 2008, 2010) and one such study analyzed only thalamo-cortical connectivity (Cho et al., 2016). In the present study, we did not constrain our exploratory investigation, and avoided a priori hypotheses or regions of interest. Thus, all the 18 tracts that could be reconstructed using TRACULA were analyzed.

Furthermore, an important feature of the current study is the well-matched homogenous sample population, which included only right-handed male participants in a narrow age range (see Table 2 for detailed demographic characteristics).

2. Methods

2.1. Participants

Thirty male UHR patients were recruited through the Mental Health Research Center (MHRC), Moscow. The UHR state was diagnosed at the time of the first visit to the MHRC, prior to treatment. We used the Scale of Prodromal Symptoms (SOPS) (Miller et al., 1999) as a diagnostic instrument, and applied criteria based on the Criteria of Prodromal States (Woods et al., 2001). Participants were assigned to the UHR group if they met the criteria of exhibiting attenuated positive symptoms (APS) and/or brief intermittent psychotic symptoms (BIPS) (further details are included in the Supplementary Methods). Additionally, the severity of depressive symptoms was measured using the Hamilton Rating Scale for Depression (HRSD). The exclusion criteria for the UHR group were: presence of true psychotic episodes, organic mental disorders, mental retardation, neurological or severe somatic disorders, and alcohol consumption or substance abuse. Mentally healthy male controls ($n = 30$) were recruited from acquaintances of the researchers and MHRC staff (demographic characteristics of both the groups are displayed in Table 2). The exclusion criteria for the control group were: presence of familial psychiatric pathology risk, severe neurological or somatic diseases, and alcohol consumption or substance abuse.

This study was approved by the Ethics Committee of the MHRC, and conformed to the Code of Ethics of the World Medical Association (Helsinki Declaration of 1975, as revised in 2008) for experiments involving humans. All the participants signed an informed consent form.

2.2. Image acquisition

All the participants underwent MRI on a 3-T Philips Achieva system (Philips, The Netherlands). The DW-MRI data were acquired using a spin- echo-planar sequence as follows: repetition time (TR) = 6657–7212 ms (depending on the number of slices, which varied with head size from 60 to 65; TR did not vary within a scan; this variation in TR did not affect the study results, as the T1-weighting factor, which is governed by TR, is divided out during the postprocessing of the DW-MRI data); echo time (TE) = 70 ms; matrix size = 144 × 144; field of view = 240 mm; one image with $b = 0$ s/mm^2 and 32 noncollinear directions with $b = 800$ s/mm^2; voxel size = 1.7 × 1.7 mm, with a slice thickness of 2 mm and no gap. The T1-weighted images were acquired using a turbo field echo sequence covering the whole brain: TR = 8.2 ms; TE = 3.7 ms; flip angle = 8°; field of view = 240 mm; and voxel size = 0.83 × 0.83 mm, with a slice thickness of 1 mm and no gap.

Table 2
Demographic and clinical information.

	UHR patients	Healthy controls	Test Statistic	*P*-value
Number	30	30	—	—
Age, mean (SD, minimum, maximum)	20.4 (2.6, 17.7, 27.6)	21.1 (2.7, 16.6, 25.4)	$t(58) = 1.05$	0.30
Gender (M/F)	30/0	30/0	—	—
Handedness: right-handed (%)	100	100	—	—
Years of education, mean (SD)	12.6 (2.0)	13.8 (2.3)	$W = 577.5$	0.06
Psychopathology scores [a], mean (SD)				
SOPS total score	41.9 (7.3)	—		
SOPS positive symptoms score	8.6 (2.9)	—		
HRSD score	20.1 (5.7)	—		
Mean antipsychotic dose, CPZ equivalent, mg/day, mean (SD)	240 (216)	—		
Total antipsychotic dose [b], CPZ equivalent, mg, mean (SD)	11,953 (11,784)	—		

CPZ, chlorpromazine.
[a] At the time of the UHR state diagnosis.
[b] Total cumulative antipsychotic dose was calculated by summing all daily doses from the first day of treatment up to MRI scan.

2.3. Image processing

2.3.1. DW-MRI

The DW-MRI data were analyzed using the TRACULA package (Yendiki et al., 2011), which uses global probabilistic tractography and incorporates anatomical priors derived from structural MR images. The overall workflow is comprised of two stages: (1) processing of T1-weighted images to obtain cortical parcellation and subcortical segmentation using the FreeSurfer software (version 5.3.0) (Fischl, 2012); and (2) preprocessing of DW-MRI data, "ball-and-stick" diffusion modelling (Behrens et al., 2007), and reconstruction of 18 pathways with computation of the FA, MD, RD, and AD values for each tract (see Supplementary Methods).

2.3.2. Structural MRI

The T1-weighted images were analyzed using the FreeSurfer software (version 5.3.0) (Fischl, 2012) to provide detailed participant-specific anatomical information. In addition to the volume-based reconstructions, FreeSurfer produces vertex-based models of the cortical surface in the native anatomical space (Dale et al., 1999; Dale and Sereno, 1993; Fischl et al., 1999a, 2004). The vertex positions were adjusted such that the surface followed the T1 intensity gradient between the cortical WM and grey matter. Smoothness constraints allowed the surface to cut through a voxel to provide subvoxel (sub-millimeter) accuracy of the surface location (Greve et al., 2013). As a result of structural image processing, the thickness, area, and volume at each vertex along each subject's brain surface were quantified (see Supplementary Methods).

2.4. Statistical analysis

Group comparisons of FA, MD, RD, and AD for each tract were performed using the R software (version 3.1.3). Multiple hypothesis testing (number of tracts analyzed) was performed with the R package "multtest" (Pollard et al., 2005), using the resampling-based procedure with the following parameters: bootstrap with centering and scaling resampling, while controlling for age; single-step, common cut-off (maxima of test statistics) multiple testing; two-sided tests with 10,000 bootstrap iterations; and a family-wise error rate of 0.05.

Vertex-wise SBM of cortical anatomy was performed using FreeSurfer's *mri_glmfit*. First, the brain surface of each subject was mapped to the standard FreeSurfer surface template *fsaverage* using a nonlinear procedure that aligns cortical folding patterns of each subject to a standard space using vertex curvature data (Fischl et al., 1999b). Cortical maps were then smoothed using a full-width-half-maximum Gaussian kernel of 10 mm. Finally, the general linear model was computed vertex-by-vertex for the analysis of group differences in cortical thickness, surface area, and cortical volume, while controlling for age. The results were corrected for multiple comparisons using a Monte-Carlo cluster-based simulation (Hagler et al., 2006), including the following steps: (1) the initial vertex-wise threshold was set to $p = 0.05$ (two-sided) to form spatially contiguous areas of association (referred to as "cluster"); and (2) the likelihood that a cluster of this size and magnitude (difference in cortical measure, as specified by the vertex-wise threshold) would appear by chance, i.e., when using repeated random sampling, was tested using Monte-Carlo simulation with 10,000 repeats. This procedure results in a cluster-wise probability (CWP), which is reported as p-value in the Results section (Section 3). In addition, CWP values were corrected for the number of hemispheres using the Bonferroni method.

The vertex-wise correlation analysis was performed using FreeSurfer's *mri_glmfit* function independently in the UHR and control groups to identify significant associations between RD in the left ATR (the only parameter that yielded significantly results in a between-group comparison, see Results) and cortical thickness, area, and volume at each vertex in the left hemisphere. We investigated associations across the entire hemisphere because it is practically impossible to accurately determine an exact cortical area where the ATR connects to cortical neurons using MRI. Statistical maps were generated by computing the general linear model of the effect of RD in the left ATR on cortical measures at each vertex, while controlling for age. The results were corrected for multiple comparisons using a Monte-Carlo simulation (see above) (Hagler et al., 2006). Additionally, we used the Spearman's rank correlation coefficient to identify correlations between RD in the left ATR and mean thickness of the left hemisphere clusters displaying significant group differences in cortical thickness.

We further conducted a correlation analysis in the R software using Spearman's rank correlation coefficients and clinical data from 26 UHR patients on the day of MRI examination (the clinical scores for 4 patients at the day of MRI were missing). Correlations were analyzed between: 1) RD in the left ATR and clinical ratings (SOPS and HRSD scores), and 2) the mean thickness of altered cortical clusters and clinical ratings (SOPS and HRSD scores). For the analysis, SOPS scores were divided into positive symptoms (SOPS-P), negative symptoms (SOPS-N), and total (SOPS-T) summarized scores. To control for the multiple comparisons of the 4 clinical scores (3 SOPS + HRSD scores) and the number of cortical clusters, Holm's sequential method (Holm, 1979) was used with the family-wise error rate controlled at 0.05.

3. Results

3.1. Demographic and clinical characteristics

Demographic and clinical characteristics of the UHR and control groups are displayed in Table 2. There were no significant differences between groups in terms of age, sex, handedness, or years of education. None of the patients received psychotropic medication at the time of UHR state diagnosis, but as determined on the day of MRI examination, 28 of the 30 UHR patients were received individually adjusted doses of antipsychotics. Among them, 4, 13, and 11 patients received typical antipsychotics, atypical antipsychotics, and both types of medication, respectively (Table 2).

3.2. WM tract diffusivity measures

Compared with controls, RD was increased in the UHR group in the left ATR ($t(56) = -2.98$, $P = 0.003$, Cohen's $d = 0.8$) (Fig. 1). No other differences between the UHR patients and controls in any of the tracts were significant following correction for multiple comparisons (Supplementary Table S1).

3.3. Cortical anatomy measures

Whole-cortex vertex-wise analysis revealed thickness reduction in the UHR patients in the parietal, temporal, frontal, and occipital cortices. Six and three clusters were located in the left and right hemispheres, respectively (Fig. 2, Table 3). Clusters with significant cortical thinning were overlaid on: (1) the Desikan atlas of gyral-based regions of interest (Desikan et al., 2006) and (2) the 7-network atlas of cortical parcellation estimated by intrinsic functional connectivity (Yeo et al., 2011) (see Table 3 for the detailed location of clusters as per gyral-based atlas). Area or volume of none of the cortical regions differed significantly between the UHR and control groups.

3.4. Associations between radial diffusivity in the left ATR and cortical thickness

We found a significant positive correlation (CWP = 0.0001) between RD in the left ATR and cortical thickness in a cluster of the left dorsolateral prefrontal cortex (DLPFC) in the UHR group (Fig. 3). There was no association between RD in the left ATR and any cortical measure

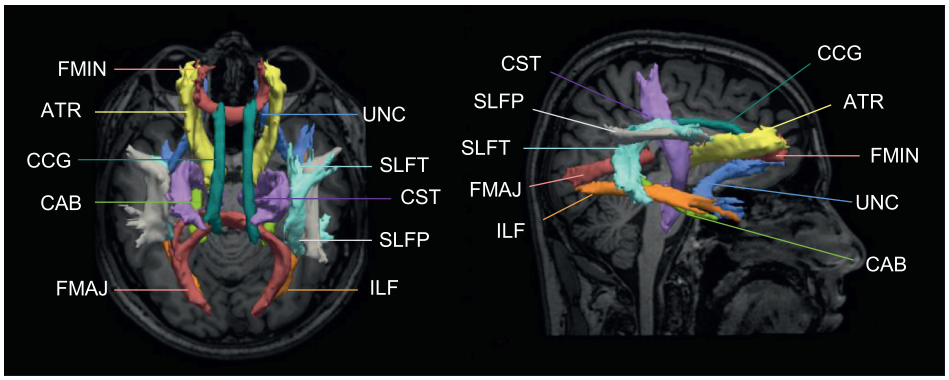

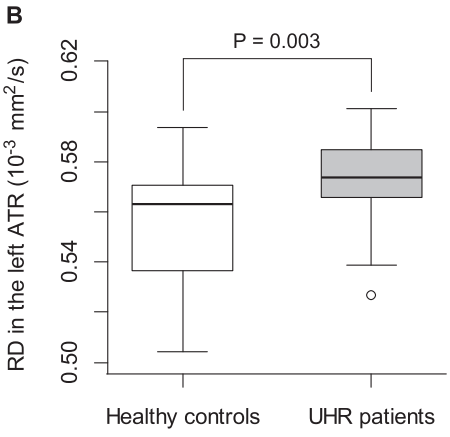

Fig. 1. (A) Example reconstruction of white matter pathways in a UHR patient. The posterior distribution of each pathway is thresholded at 20% of its maximum and displayed as an isosurface over the patient's T1-weighted image (axial and sagittal projections). CST, corticospinal tract; ILF, inferior longitudinal fasciculus; UNC, uncinate fasciculus; ATR, anterior thalamic radiation; CCG, cingulum—cingulate gyrus (supracallosal) bundle; CAB, cingulum—angular (infracallosal) bundle; SLFP, superior longitudinal fasciculus— parietal bundle; SLFT, superior longitudinal fasciculus—temporal bundle; FMAJ, corpus callosum— forceps major; FMIN, corpus callosum—forceps minor. (B) Boxplot of RD in the left ATR by groups.

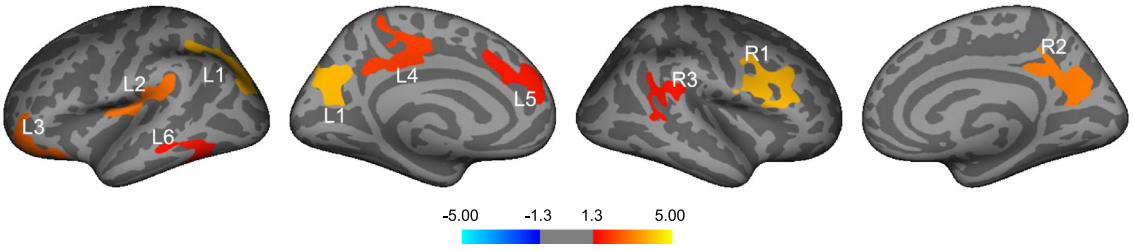

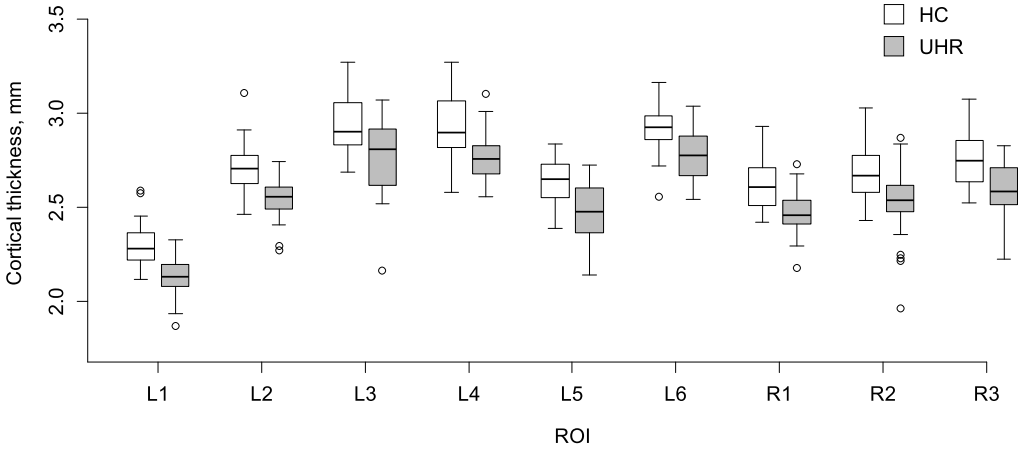

Fig. 2. Surface statistical maps and boxplots displaying clusters of cortical thickness reductions in UHR patients compared to controls. Clusters are mapped onto the inflated standard FreeSurfer cortical template, where light grey indicates a gyrus and dark grey indicates a sulcus. Cluster-wise probability values (corrected for multiple comparisons) are represented according to the colour scale bar showing the logarithmic scale of *p*-values ($-\log(10)p$).

Table 3
Localization, size and CWP of cortical thinning clusters in the UHR group compared to the control group.

Cluster	Localization as per Desikan atlas (Desikan et al., 2006), anatomical labels [a]	Localization as per intrinsic functional connectivity atlas (Yeo et al., 2011), networks [a]	Size, mm^2	CWP * (df = 56)	Cohen's *d*
Left hemisphere					
1	Superior parietal, inferior parietal, precuneus, cuneus	Frontoparietal control, default, dorsal attention, visual	3137	0.0001	1.60
2	Supramarginal, insula	Ventral attention, somatomotor,	1251	0.0011	1.35
3	Rostral middle frontal, inferior frontal (pars orbitalis), orbital frontal	Default, frontoparietal control	1203	0.0015	0.96
4	ParaCentral lobule, posterior cingulate, precuneus, isthmus	Default, ventral attention	1007	0.0064	1.11
5	Medial superior frontal	Default, frontoparietal control, ventral attention	848	0.0207	1.11
6	Inferior temporal, middle temporal	Default, frontoparietal control, dorsal attention	822	0.0241	1.15
Right hemisphere					
1	Pre central, inferior frontal (pars opercularis and pars triangularis) rostral middle frontal, caudal middle frontal	Frontoparietal control, dorsal attention, ventral attention	1783	0.0001	1.14
2	PreCuneus, isthmus	Default, frontoparietal control, visual	1280	0.0008	0.95
3	Supramarginal, inferior parietal	Default, ventral attention	863	0.0238	1.20

[a] List of labels and networks that intersect a cluster.
* CWP: cluster-wise probability fully corrected for multiple comparisons, all listed CWPs remained significant after controlling for multiple comparisons corresponding to the number of hemispheres using the Bonferroni method.

in the UHR or control groups. There were also no correlations between RD in the left ATR and the thickness of any of the left hemisphere clusters that corresponded to significant group differences in cortical thickness.

3.5. Correlation analysis

No significant correlations among RD in the left ATR, reduced cortical thickness, and clinical scores were revealed. Additionally, correlation analysis was performed to examine whether RD in the left ATR or reduced cortical thickness were associated with chlorpromazine-equivalent doses (daily and total), and no associations were found.

4. Discussion

To the best of our knowledge, the present study is the first to apply a multimodal design of automated, rater-independent, and validated approaches (Fischl et al., 2008; Kuperberg et al., 2003; Rosas et al., 2002; Sarica et al., 2014) for tractography and cortex surface reconstruction in UHR subjects.

4.1. Microstructural abnormalities in the left ATR

The only difference between the UHR and control groups was the increased RD in the left ATR. The ATR passes through the anterior limb of the internal capsule and connects the dorsomedial and anterior thalamic nuclei with the prefrontal cortex (PFC), most likely with its dorsolateral region (Coenen et al., 2012). Therefore, the ATR is presumably a part of the dorsolateral prefrontal-subcortical circuit (Middleton and Strick, 2001), functional and structural deficits in which may be related to the cognitive impairments in schizophrenia (Sui et al., 2015). Several studies have revealed reduction in the thalamo-prefrontal functional connectivity in both UHR and schizophrenia patients (Anticevic et al., 2015; Giraldo-Chica and Woodward, 2017), which could be linked to structural connectivity abnormalities in the ATR (Marenco et al., 2012), characterized, among other things, by increased radial diffusivity (Squarcina et al., 2017; Zeng et al., 2016). The ATR also interconnects the DLPFC and the hippocampus (Coenen et al., 2012), and this hippocampal-DLPFC coupling may represent a systems-level mechanism that is specific to spatial working memory (Bahner et al., 2015) which has been consistently reported to be impaired in UHR patients (Bora et al., 2014).

Based on the present knowledge of the physiological nature of diffusion changes in the WM (Aung et al., 2013; Song et al., 2005; Sun et al., 2006), increased RD in the left ATR could be a consequence of myelin pathology as it allows increased water diffusion perpendicular to axons, while unchanged AD may indicate an absence of axonal damage. However, it is not yet clear whether this pattern might indicate myelin degradation or pathological aberration (delay or deficient) of myelination in UHR patients compared with controls (Mighdoll et al., 2015), and remains to be elucidated via further longitudinal studies (Krakauer et al., 2018; Maas et al., 2017).

It is difficult to directly compare the observed RD alteration with the results of other DW-MRI UHR studies, as only 4 of them have analyzed this diffusivity measure. Three voxel-based studies have reported negative results for RD (Carletti et al., 2012; Krakauer et al., 2017; Wang et al., 2016a) (although Wang et al. (2016a) and Krakauer et al. (2017) reported reduced FA in the left ATR), and one reported increased RD in the right posterior corona radiata, with no FA changes (von Hohenberg et al., 2014). Furthermore, sex differences could be considered a factor

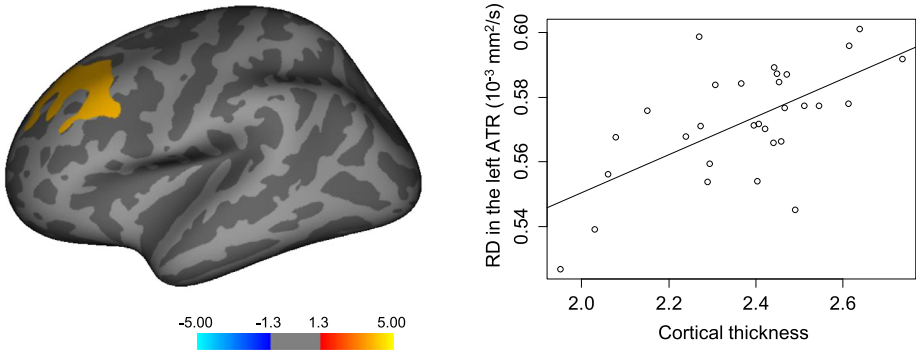

Fig. 3. Cortical statistical maps and scatter plot displaying positive associations between RD in the left ATR and cortical thickness in UHR individuals. Clusters are mapped onto the inflated standard FreeSurfer cortical template, where light grey indicates a gyrus and dark grey indicates a sulcus. Cluster-wise probability values (corrected for multiple comparisons) are represented according to the colour scale bar showing the logarithmic scale of *p*-values (−log(10)p).

contributing to the discrepancies between the present and previous studies, which included 28–51% female participants (Carletti et al., 2012; Krakauer et al., 2017; von Hohenberg et al., 2014; Wang et al., 2016a). This may be important as RD changes during development have been shown to differ between sexes (Kumar et al., 2012). Two tractography studies (Peters et al., 2008, 2010) did not examine either ATR or RD and did not find FA reduction in other tracts, and one found post-hoc FA reduction in the fascicle connecting the thalamus and orbitofrontal cortex (Cho et al., 2016), which is presumably a part of the ATR (Coenen et al., 2012).

4.2. Cortical thickness reduction

We confirmed previous findings by demonstrating reduced cortical thickness in the frontal, temporal, and parietal areas in the UHR patients (Benetti et al., 2013; Gisselgard et al., 2018; Jung et al., 2011; Kwak et al., 2018; Takayanagi et al., 2017) (see Table 3 for the specific anatomical location of clusters as per gyral-based Desikan atlas). Such widespread impairments in cortical anatomy may be associated with deficits in various cognitive domains. Indeed, it has been shown that cognitive deficits in UHR patients may be subserved by structurally altered brain regions (Koutsouleris et al., 2010) and by abnormal brain function directly related to such structural alterations (Fusar-Poli et al., 2011b). Considering this, cortical thinning in the left precuneus, superior parietal lobule, and right middle and inferior frontal gyri may be linked to working memory impairments in UHR patients (Falkenberg et al., 2017; Fusar-Poli et al., 2010; Schmidt et al., 2014). Grey matter alterations in the left supramarginal gyrus, inferior parietal lobule, and middle frontal gyrus may also be linked to working memory. Moreover, reduced prefrontal activation during a working memory task in UHR patients is directly associated with reduced grey matter volume in the same area (Fusar-Poli et al., 2011b). Structural abnormalities in the PFC in UHR patients have also been reported to be associated with executive deficits (Koutsouleris et al., 2010) and meta-cognitive functions (Buchy et al., 2015). Other regions showing cortical thinning include parts of the ventromedial prefrontal, medial prefrontal, premotor, and posterior cingulate cortices, and the insula, all of which are implicated in social cognition (Adolphs, 2009). Abnormalities in these cortical areas may underlie the cognitive deficits that are exhibited in all social cognition domains in UHR patients (Lee et al., 2015; Lincoln et al., 2017). For example, it has been reported that functional connectivity between the posterior cingulate cortex and several brain regions is correlated with facial emotion recognition performance in a UHR group (Pelletier-Baldelli et al., 2015).

However, it is important to note that direct comparison of the current study results (all-male study population) with the results of the other SBM UHR studies is difficult due to sex differences. Although the most of the previous UHR studies have not analyzed sex-by-group interactions involving cortical thickness (Bakker et al., 2016; Benetti et al., 2013; Cannon et al., 2015; Gisselgard et al., 2018; Haller et al., 2009; Jung et al., 2011; Klauser et al., 2015; Kwak et al., 2018; Takayanagi et al., 2017; Tognin et al., 2014; Ziermans et al., 2012), a recent UHR study has shown significant sex-by-group interactions with opposite directions of effect in male and female UHR patients in multiple cortical areas (Guma et al., 2017). It is difficult to state the cause of such neuroanatomical sex differences in UHR patients, but there is a possibility that it may be associated with variations in symptomatology in men and women with psychotic symptoms (Guma et al., 2017; Rietschel et al., 2017). As the main limitation of the mentioned study is its small sample size (13 male and 13 female UHR patients) (Guma et al., 2017), potential sex-by-group interactions involving cortical thickness remains to be clarified via further research on UHR. This is especially true since the ENIGMA meta-analysis of cortical thickness abnormalities in schizophrenia using a large sample population of 4474 individuals did not reveal any significant group-by-sex interactions involving cortical thickness (van Erp et al., 2018).

Considering the network nature of brain architecture, it is important to note that all revealed cortical clusters overlapped with areas of the default, frontoparietal control, and ventral or dorsal attention networks (see Table 3 for the detailed location of clusters as per intrinsic functional connectivity atlas (Yeo et al., 2011)). The UHR patients have been reported to exhibit abnormal connectivity within the default and control networks (Colibazzi et al., 2016; Shim et al., 2010), and reduced anticorrelations between the default network nodes and control or task-related areas (Fryer et al., 2013; Shim et al., 2010; Wotruba et al., 2014), which may indicate deficient task-related network capacity for appropriate cognitive processing. Considering a direct relationship between altered brain function and structural abnormalities in UHR patients (Fusar-Poli et al., 2011b), it may be suggested that dysfunction of intrinsic networks might develop with cortical thickness abnormalities and account for the widespread cognitive deficits observed in UHR patients (Mam-Lam-Fook et al., 2017). However, there are no multimodal studies regarding associations among cortical anatomy, functional connectivity, and neurocognitive functioning in UHR patients, thus presenting avenues for future research.

The revealed alterations in the left ATR microstructure might also support the hypothesis of default and task-related networks dysregulation in the UHR state. Indeed, the ATR connects the mediodorsal and anterior thalamus with the prefrontal areas of both default and control networks (Coenen et al., 2012; Yeo et al., 2011). Furthermore, the mediodorsal nuclei are hypothesized to be among the central components of cortico-thalamo-cortical circuits, providing the means whereby different cortical areas, including the control or default mode networks, cooperate for various cognitive functions (Dwyer et al., 2014; Sherman, 2016). Importantly, a pattern of structural and functional hypoconnectivity between the thalamus and PFC has been detected in both schizophrenia and UHR patients (Anticevic et al., 2015; Cho et al., 2016; Giraldo-Chica et al., 2018; Giraldo-Chica and Woodward, 2017; Wang et al., 2016a). These findings might indicate that the revealed abnormal structural connectivity between the thalamus and the PFC in UHR patients could be implicated in the imbalanced interplay between the default and task-related networks. However, future multimodal research (using functional MRI and DWI-MRI) is needed to elucidate such potential implications and the relationship between the mentioned alterations in functional and anatomical connectivity.

4.3. Associations between radial diffusivity in the left ATR and cortical thickness

We hypothesized that the disturbed WM microstructure would be associated with decreased cortical thickness, as has been previously reported in schizophrenia patients (Koch et al., 2013; Kubota et al., 2013; Sasamoto et al., 2014); however, the results did not confirm this hypothesis (for a list of some issues that might have potentially reduced the sensitivity of the methods used in this study to detect such associations, see Section 4.5 [Limitations]). In contrast, a positive correlation between abnormal WM microstructure in the left ATR and unaltered cortical thickness in an adjacent DLPFC area was identified, which is similar to the associations reported in healthy subjects in the same cortical area (Tamnes et al., 2010). However, there were no associations between RD in the left ATR and cortical thickness in our control group. One potential explanation is that the age range of our control group was much narrower than that of the aforementioned study (Tamnes et al., 2010), thus hindering the possible detection of statistically significant correlations. In summary, the findings of the present cross-sectional study suggest that WM and grey matter abnormalities are not directly interrelated in the UHR state. However, whether such associations occur before or after psychosis onset is not yet clear and remains to be elucidated via further longitudinal research, which will allow the investigation of individuals who later convert to psychosis.

4.4. Correlations with clinical data

There were no significant correlations among RD in the left ATR, reduced cortical thickness, and SOPS or HRDS scores. This finding corresponds to the results of other DW-MRI (Peters et al., 2008; von Hohenberg et al., 2014) and SBM (Benetti et al., 2013; Jung et al., 2011; Takayanagi et al., 2017; van Lutterveld et al., 2014) studies in UHR patients. One speculative interpretation is that the psychopathology may be associated with a complex system of structural and functional impairments and intact brain circuits, rather than directly correlating with structural changes in separate cortical regions or WM fascicles. However, some studies have found that the thalamo-OFC relative connectivity and FA in the left inferior longitudinal fasciculus are positively correlated with the level of functioning in UHR patients (Cho et al., 2016; Krakauer et al., 2017), and that the reduced thickness in the left PFC and right inferior parietal lobule is correlated with more severe SOPS general and disorganization symptom scores, respectively (Kwak et al., 2018). Therefore, it is possible that the clinical scores and methods used in this study were not sufficiently sensitive to detect such associations due to some limitations (see Section 4.5 [Limitations]).

4.5. Limitations

Several potential limitations of the present study should be considered. First, although homogeneity of the UHR group (in terms of sex, age, and handedness) is a strength of the current study, such a sample population limits the degree to which the findings can be generalized to other populations in view of potential sex-by-group interactions involving DW-MRI findings or cortical thickness measures in UHR patients (Guma et al., 2017; Kumar et al., 2012). Second, we did not identify any association between WM and grey matter abnormalities or between anatomy and clinical data in the UHR group. However, it is possible that the methods used in this study were not sufficiently sensitive to detect such subtle relationship due to the modest sample size, limited number of noncollinear directions, voxel size, and non-isotropic voxel DW-MRI sequence. Third, while we found no correlations between WM and grey matter alterations and chlorpromazine equivalent doses in the UHR group, it is impossible to fully exclude potential medication effects on the revealed abnormalities. To date, studies on this topic have yielded inconsistent results. It has been previously shown that first-episode psychosis patients (FEP) demonstrated reduced FA (Wang et al., 2013) and increased RD (Szeszko et al., 2014) following atypical antipsychotic treatment, although the FA decrease did not correlate with medication dose (Wang et al., 2013). Further, studies in neuroleptic-naïve UHR (Peters et al., 2009; Wang et al., 2016a) and FEP (Alvarado-Alanis et al., 2015; Cheung et al., 2011; Lei et al., 2015; Mandl et al., 2013; Serpa et al., 2017; Sun et al., 2015) patients have revealed that FA reduction (including reduction in the left ATR (Serpa et al., 2017; Wang et al., 2016a)) is not attributable to medication, while a longitudinal study showed that FA increase and corresponding RD decrease are positively correlated with antipsychotic exposure in FEP patients (Reis Marques et al., 2014). The longitudinal UHR study revealed reduced FA in the same region in UHR patients who were not prescribed antipsychotics and in those treated with antipsychotics, and comparison of FA between these two subgroups did not show significant effects of group, time, or time × group interaction, suggesting that the revealed FA reduction is not attributable to medication (Katagiri et al., 2015). Moreover, the largest coordinated study of WM differences in schizophrenia to date detected no significant impact of antipsychotic medication on FA changes in patients, suggesting that regardless of the causes, their effects do not overlap exclusively with a treatment (Kelly et al., 2017). In addition, it has been reported that quetiapine (an atypical antipsychotic) stimulates neural progenitor cell proliferation and oligodendrocyte differentiation, and facilitates myelination (Xiao et al., 2008), whereas haloperidol (a typical antipsychotic) has been reported to promote proliferation but inhibit differentiation in rat oligodendrocyte progenitor cell culture (Niu et al., 2010), suggesting that different types of antipsychotics may exert opposite effects on WM microstructure integrity. Studies exploring the influence of antipsychotic medication on cortical thickness have also shown inconsistent results. A previous study reported cortical thinning in FEP patients treated with atypical antipsychotics compared with healthy controls and unmedicated patients (Lesh et al., 2015), while another study showed that cortical thickness increased over 8 weeks of atypical antipsychotic therapy in FEP patients (Goghari et al., 2013). Two recent studies have analyzed the potential associations between antipsychotic dosage and cortical thickness, one of which revealed an association (Moser et al., 2018), while the other did not (Walton et al., 2018). Cortical thinning has recently been shown to occur in non-medicated UHR (Gisselgard et al., 2018; Kwak et al., 2018) and neuroleptic-naïve FEP patients (Song et al., 2015; Xiao et al., 2015). Voxel-based meta-analyses has revealed that antipsychotic-naive UHR patients show consistent grey matter reductions (Fusar-Poli et al., 2012); moreover, UHR patients who received atypical antipsychotic treatment show increase in grey matter volume compared with antipsychotic-naive UHR patients (Fusar-Poli et al., 2011a). Furthermore, recent studies have shown that first- and second-generation antipsychotics may exert contrasting effects on cortical thickness (Ansell et al., 2015) and cortical grey matter volume (Vita et al., 2015). In total, the exact influence of antipsychotic medication on diffusivity measures and cortical thickness is not yet clear and remains to be elucidated via further research.

4.6. Conclusion

The findings of the present study suggest that the UHR state is associated with cortical thickness reductions in the brain regions presumably involved in processing and coordinating external and internal information streams and structural connectivity alterations in the left ATR, likely caused by myelin pathology. Such structural abnormalities may, in turn, underlie widespread deficits in neurocognitive and social functioning, which is consistently reported in UHR patients. Finally, the results suggest that WM microstructure and cortical thickness abnormalities are not directly related in UHR patients in contrast to the pathological patterns reported in schizophrenia patients.

Acknowledgment

This work was supported by a research grant from the Russian Humanitarian Foundation (grant code 13-06-00655).

Declaration of interest

None.

Supplementary materials

Supplementary material associated with this article can be found, in the online version, at doi:https://doi.org/10.1016/j.pscychresns.2019.05.002.

References

Adolphs, R., 2009. The social brain: neural basis of social knowledge. Annu. Rev. Psychol. 60, 693–716.

Alvarado-Alanis, P., Leon-Ortiz, P., Reyes-Madrigal, F., Favila, R., Rodriguez-Mayoral, O., Nicolini, H., Azcarraga, M., Graff-Guerrero, A., Rowland, L.M., de la Fuente-Sandoval, C., 2015. Abnormal white matter integrity in antipsychotic-naive first-episode psychosis patients assessed by a DTI principal component analysis. Schizophr. Res. 162, 14–21.

Ansell, B.R., Dwyer, D.B., Wood, S.J., Bora, E., Brewer, W.J., Proffitt, T.M., Velakoulis, D., McGorry, P.D., Pantelis, C., 2015. Divergent effects of first-generation and second-generation antipsychotics on cortical thickness in first-episode psychosis. Psychol. Med. 45, 515–527.

Anticevic, A., Haut, K., Murray, J.D., Repovs, G., Yang, G.J., Diehl, C., McEwen, S.C.,

Bearden, C.E., Addington, J., Goodyear, B., Cadenhead, K.S., Mirzakhanian, H., Cornblatt, B.A., Olvet, D., Mathalon, D.H., McGlashan, T.H., Perkins, D.O., Belger, A., Seidman, L.J., Tsuang, M.T., van Erp, T.G., Walker, E.F., Hamann, S., Woods, S.W., Qiu, M., Cannon, T.D., 2015. Association of thalamic dysconnectivity and conversion to psychosis in youth and young adults at elevated clinical risk. JAMA Psychiatry 72, 882–891.

Aung, W.Y., Mar, S., Benzinger, T.L., 2013. Diffusion tensor MRI as a biomarker in axonal and myelin damage. Imaging Med. 5, 427–440.

Bahner, F., Demanuele, C., Schweiger, J., Gerchen, M.F., Zamoscik, V., Ueltzhoffer, K., Hahn, T., Meyer, P., Flor, H., Durstewitz, D., Tost, H., Kirsch, P., Plichta, M.M., Meyer-Lindenberg, A., 2015. Hippocampal-dorsolateral prefrontal coupling as a species-conserved cognitive mechanism: a human translational imaging study. Neuropsychopharmacology 40, 1674–1681.

Bakker, G., Caan, M.W., Vingerhoets, W.A., da Silva-Alves, F., de Koning, M., Boot, E., Nieman, D.H., de Haan, L., Bloemen, O.J., Booij, J., van Amelsvoort, T.A., 2016. Cortical morphology differences in subjects at increased vulnerability for developing a psychotic disorder: a comparison between subjects with ultra-high risk and 22q11.2 deletion syndrome. PLoS One 11, e0159928.

Bartholomeusz, C.F., Cropley, V.L., Wannan, C., Di Biase, M., McGorry, P.D., Pantelis, C., 2017. Structural neuroimaging across early-stage psychosis: aberrations in neurobiological trajectories and implications for the staging model. Aust. N. Z. J. Psychiatry 51, 455–476.

Behrens, T.E., Berg, H.J., Jbabdi, S., Rushworth, M.F., Woolrich, M.W., 2007. Probabilistic diffusion tractography with multiple fibre orientations: what can we gain? Neuroimage 34, 144–155.

Benetti, S., Pettersson-Yeo, W., Hutton, C., Catani, M., Williams, S.C., Allen, P., Kambeitz-Ilankovic, L.M., McGuire, P., Mechelli, A., 2013. Elucidating neuroanatomical alterations in the at risk mental state and first episode psychosis: a combined voxel-based morphometry and voxel-based cortical thickness study. Schizophr. Res. 150, 505–511.

Bloemen, O.J., de Koning, M.B., Schmitz, N., Nieman, D.H., Becker, H.E., de Haan, L., Dingemans, P., Linszen, D.H., van Amelsvoort, T.A., 2010. White-matter markers for psychosis in a prospective ultra-high-risk cohort. Psychol. Med. 40, 1297–1304.

Bois, C., Whalley, H.C., McIntosh, A.M., Lawrie, S.M., 2015. Structural magnetic resonance imaging markers of susceptibility and transition to schizophrenia: a review of familial and clinical high risk population studies. J. Psychopharmacol. 29, 144–154.

Bora, E., Lin, A., Wood, S.J., Yung, A.R., McGorry, P.D., Pantelis, C., 2014. Cognitive deficits in youth with familial and clinical high risk to psychosis: a systematic review and meta-analysis. Acta Psychiatr. Scand. 130, 1–15.

Brent, B.K., Thermenos, H.W., Keshavan, M.S., Seidman, L.J., 2013. Gray matter alterations in schizophrenia high-risk youth and early-onset schizophrenia: a review of structural MRI findings. Child Adolesc. Psychiatr. Clin. N. Am. 22, 689–714.

Buchy, L., Stowkowy, J., MacMaster, F.P., Nyman, K., Addington, J., 2015. Meta-cognition is associated with cortical thickness in youth at clinical high risk of psychosis. Psychiatry Res. 233, 418–423.

Cannon, T.D., Chung, Y., He, G., Sun, D., Jacobson, A., van Erp, T.G., McEwen, S., Addington, J., Bearden, C.E., Cadenhead, K., Cornblatt, B., Mathalon, D.H., McGlashan, T., Perkins, D., Jeffries, C., Seidman, L.J., Tsuang, M., Walker, E., Woods, S.W., Heinssen, R., North American Prodrome Longitudinal Study, C., 2015. Progressive reduction in cortical thickness as psychosis develops: a multisite longitudinal neuroimaging study of youth at elevated clinical risk. Biol. Psychiatry 77, 147–157.

Carletti, F., Woolley, J.B., Bhattacharyya, S., Perez-Iglesias, R., Fusar Poli, P., Valmaggia, L., Broome, M.R., Bramon, E., Johns, L., Giampietro, V., Williams, S.C., Barker, G.J., McGuire, P.K., 2012. Alterations in white matter evident before the onset of psychosis. Schizophr. Bull. 38, 1170–1179.

Cheung, V., Chiu, C.P., Law, C.W., Cheung, C., Hui, C.L., Chan, K.K., Sham, P.C., Deng, M.Y., Tai, K.S., Khong, P.L., McAlonan, G.M., Chua, S.E., Chen, E., 2011. Positive symptoms and white matter microstructure in never-medicated first episode schizophrenia. Psychol. Med. 41, 1709–1719.

Cho, K.I., Shenton, M.E., Kubicki, M., Jung, W.H., Lee, T.Y., Yun, J.Y., Kim, S.N., Kwon, J.S., 2016. Altered thalamo-cortical white matter connectivity: probabilistic tractography study in clinical-high risk for psychosis and first-episode psychosis. Schizophr. Bull. 42, 723–731.

Coenen, V.A., Panksepp, J., Hurwitz, T.A., Urbach, H., Madler, B., 2012. Human medial forebrain bundle (MFB) and anterior thalamic radiation (ATR): imaging of two major subcortical pathways and the dynamic balance of opposite affects in understanding depression. J. Neuropsychiatry Clin. Neurosci. 24, 223–236.

Colibazzi, T., Horga, G., Wang, Z., Huo, Y., Corcoran, C., Klahr, K., Brucato, G., Girgis, R., Gill, K., Abi-Dargham, A., Peterson, B.S., 2016. Neural dysfunction in cognitive control circuits in persons at clinical high-risk for psychosis. Neuropsychopharmacology 41, 1241–1250.

Dale, A.M., Fischl, B., Sereno, M.I., 1999. Cortical surface-based analysis. I. Segmentation and surface reconstruction. Neuroimage 9, 179–194.

Dale, A.M., Sereno, M.I., 1993. Improved localization of cortical activity by combining EEG and MEG with MRI cortical surface reconstruction: a linear approach. J. Cogn. Neurosci. 5, 162–176.

Desikan, R.S., Segonne, F., Fischl, B., Quinn, B.T., Dickerson, B.C., Blacker, D., Buckner, R.L., Dale, A.M., Maguire, R.P., Hyman, B.T., Albert, M.S., Killiany, R.J., 2006. An automated labeling system for subdividing the human cerebral cortex on MRI scans into gyral based regions of interest. Neuroimage 31, 968–980.

Dukart, J., Smieskova, R., Harrisberger, F., Lenz, C., Schmidt, A., Walter, A., Huber, C., Riecher-Rossler, A., Simon, A., Lang, U.E., Fusar-Poli, P., Borgwardt, S., 2017. Age-related brain structural alterations as an intermediate phenotype of psychosis. J. Psychiatry Neurosci. 42, 307–319.

Dwyer, D.B., Harrison, B.J., Yucel, M., Whittle, S., Zalesky, A., Pantelis, C., Allen, N.B., Fornito, A., 2014. Large-scale brain network dynamics supporting adolescent cognitive control. J. Neurosci. 34, 14096–14107.

Falkenberg, I., Valli, I., Raffin, M., Broome, M.R., Fusar-Poli, P., Matthiasson, P., Picchioni, M., McGuire, P., 2017. Pattern of activation during delayed matching to sample task predicts functional outcome in people at ultra high risk for psychosis. Schizophr. Res. 181, 86–93.

Fischl, B., 2012. FreeSurfer. Neuroimage 62, 774–781.

Fischl, B., Rajendran, N., Busa, E., Augustinack, J., Hinds, O., Yeo, B.T., Mohlberg, H., Amunts, K., Zilles, K., 2008. Cortical folding patterns and predicting cytoarchitecture. Cereb. Cortex 18, 1973–1980.

Fischl, B., Sereno, M.I., Dale, A.M., 1999a. Cortical surface-based analysis. II: inflation, flattening, and a surface-based coordinate system. Neuroimage 9, 195–207.

Fischl, B., Sereno, M.I., Tootell, R.B., Dale, A.M., 1999b. High-resolution intersubject averaging and a coordinate system for the cortical surface. Hum. Brain Mapp. 8, 272–284.

Fischl, B., van der Kouwe, A., Destrieux, C., Halgren, E., Segonne, F., Salat, D.H., Busa, E., Seidman, L.J., Goldstein, J., Kennedy, D., Caviness, V., Makris, N., Rosen, B., Dale, A.M., 2004. Automatically parcellating the human cerebral cortex. Cereb. Cortex 14, 11–22.

Fornito, A., Yung, A.R., Wood, S.J., Phillips, L.J., Nelson, B., Cotton, S., Velakoulis, D., McGorry, P.D., Pantelis, C., Yucel, M., 2008. Anatomic abnormalities of the anterior cingulate cortex before psychosis onset: an MRI study of ultra-high-risk individuals. Biol. Psychiatry 64, 758–765.

Fryer, S.L., Woods, S.W., Kiehl, K.A., Calhoun, V.D., Pearlson, G.D., Roach, B.J., Ford, J.M., Srihari, V.H., McGlashan, T.H., Mathalon, D.H., 2013. Deficient suppression of default mode regions during working memory in individuals with early psychosis and at clinical high-risk for psychosis. Front. Psychiatry 4, 92.

Fusar-Poli, P., Borgwardt, S., Bechdolf, A., Addington, J., Riecher-Rossler, A., Schultze-Lutter, F., Keshavan, M., Wood, S., Ruhrmann, S., Seidman, L.J., Valmaggia, L., Cannon, T., Velthorst, E., De Haan, L., Cornblatt, B., Bonoldi, I., Birchwood, M., McGlashan, T., Carpenter, W., McGorry, P., Klosterkotter, J., McGuire, P., Yung, A., 2013. The psychosis high-risk state: a comprehensive state-of-the-art review. JAMA Psychiatry 70, 107–120.

Fusar-Poli, P., Borgwardt, S., Crescini, A., Deste, G., Kempton, M.J., Lawrie, S., Mc Guire, P., Sacchetti, E., 2011a. Neuroanatomy of vulnerability to psychosis: a voxel-based meta-analysis. Neurosci. Biobehav. Rev. 35, 1175–1185.

Fusar-Poli, P., Broome, M.R., Matthiasson, P., Woolley, J.B., Johns, L.C., Tabraham, P., Bramon, E., Valmaggia, L., Williams, S.C., McGuire, P., 2010. Spatial working memory in individuals at high risk for psychosis: longitudinal fMRI study. Schizophr. Res. 123, 45–52.

Fusar-Poli, P., Broome, M.R., Woolley, J.B., Johns, L.C., Tabraham, P., Bramon, E., Valmaggia, L., Williams, S.C., McGuire, P., 2011b. Altered brain function directly related to structural abnormalities in people at ultra high risk of psychosis: longitudinal VBM-fMRI study. J. Psychiatr. Res. 45, 190–198.

Fusar-Poli, P., Radua, J., McGuire, P., Borgwardt, S., 2012. Neuroanatomical maps of psychosis onset: voxel-wise meta-analysis of antipsychotic-naive VBM studies. Schizophr. Bull. 38, 1297–1307.

Giorgio, A., Watkins, K.E., Douaud, G., James, A.C., James, S., De Stefano, N., Matthews, P.M., Smith, S.M., Johansen-Berg, H., 2008. Changes in white matter microstructure during adolescence. Neuroimage 39, 52–61.

Giraldo-Chica, M., Rogers, B.P., Damon, S.M., Landman, B.A., Woodward, N.D., 2018. Prefrontal-thalamic anatomical connectivity and executive cognitive function in schizophrenia. Biol. Psychiatry 83, 509–517.

Giraldo-Chica, M., Woodward, N.D., 2017. Review of thalamocortical resting-state fMRI studies in schizophrenia. Schizophr. Res. 180, 58–63.

Gisselgard, J., Lebedev, A.V., Daehli Kurz, K., Joa, I., Johannessen, J.O., Bronnick, K., 2018. Structural and functional alterations in the brain during working memory in medication-naive patients at clinical high-risk for psychosis. PLoS One 13, e0196289.

Goghari, V.M., Smith, G.N., Honer, W.G., Kopala, L.C., Thornton, A.E., Su, W., Macewan, G.W., Lang, D.J., 2013. Effects of eight weeks of atypical antipsychotic treatment on middle frontal thickness in drug-naive first-episode psychosis patients. Schizophr. Res. 149, 149–155.

Greve, D.N., Van der Haegen, L., Cai, Q., Stufflebeam, S., Sabuncu, M.R., Fischl, B., Brysbaert, M., 2013. A surface-based analysis of language lateralization and cortical asymmetry. J. Cogn. Neurosci. 25, 1477–1492.

Guma, E., Devenyi, G.A., Malla, A., Shah, J., Chakravarty, M.M., Pruessner, M., 2017. Neuroanatomical and symptomatic sex differences in individuals at clinical high risk for psychosis. Front. Psychiatry 8, 291.

Hagler Jr., D.J., Saygin, A.P., Sereno, M.I., 2006. Smoothing and cluster thresholding for cortical surface-based group analysis of fMRI data. Neuroimage 33, 1093–1103.

Haller, S., Borgwardt, S.J., Schindler, C., Aston, J., Radue, E.W., Riecher-Rössler, A., 2009. Can cortical thickness asymmetry analysis contribute to detection of at-risk mental state and first-episode psychosis? A pilot study. Radiology 250, 212–221.

Hilgetag, C.C., Barbas, H., 2006. Role of mechanical factors in the morphology of the primate cerebral cortex. PLoS Comput. Biol. 2, e22.

Holm, S., 1979. A simple sequentially rejective multiple test procedure. Scand. J. Stat. 6, 65–70.

Jung, W.H., Kim, J.S., Jang, J.H., Choi, J.S., Jung, M.H., Park, J.Y., Han, J.Y., Choi, C.H., Kang, D.H., Chung, C.K., Kwon, J.S., 2011. Cortical thickness reduction in individuals at ultra-high-risk for psychosis. Schizophr. Bull. 37, 839–849.

Karlsgodt, K.H., Niendam, T.A., Bearden, C.E., Cannon, T.D., 2009. White matter integrity and prediction of social and role functioning in subjects at ultra-high risk for psychosis. Biol. Psychiatry 66, 562–569.

Katagiri, N., Pantelis, C., Nemoto, T., Zalesky, A., Hori, M., Shimoji, K., Saito, J., Ito, S., Dwyer, D.B., Fukunaga, I., Morita, K., Tsujino, N., Yamaguchi, T., Shiraga, N., Aoki,

S., Mizuno, M., 2015. A longitudinal study investigating sub-threshold symptoms and white matter changes in individuals with an 'at risk mental state' (ARMS). Schizophr. Res. 162, 7–13.
Kelly, S., Jahanshad, N., Zalesky, A., Kochunov, P., Agartz, I., Alloza, C., Andreassen, O.A., Arango, C., Banaj, N., Bouix, S., Bousman, C.A., Brouwer, R.M., Bruggemann, J., Bustillo, J., Cahn, W., Calhoun, V., Cannon, D., Carr, V., Catts, S., Chen, J., Chen, J.X., Chen, X., Chiapponi, C., Cho, K.K., Ciullo, V., Corvin, A.S., Crespo-Facorro, B., Cropley, V., De Rossi, P., Diaz-Caneja, C.M., Dickie, E.W., Ehrlich, S., Fan, F.M., Faskowitz, J., Fatouros-Bergman, H., Flyckt, L., Ford, J.M., Fouche, J.P., Fukunaga, M., Gill, M., Glahn, D.C., Gollub, R., Goudzwaard, E.D., Guo, H., Gur, R.E., Gur, R.C., Gurholt, T.P., Hashimoto, R., Hatton, S.N., Henskens, F.A., Hibar, D.P., Hickie, I.B., Hong, L.E., Horacek, J., Howells, F.M., Hulshoff Pol, H.E., Hyde, C.L., Isaev, D., Jablensky, A., Jansen, P.R., Janssen, J., Jonsson, E.G., Jung, L.A., Kahn, R.S., Kikinis, Z., Liu, K., Klauser, P., Knochel, C., Kubicki, M., Lagopoulos, J., Langen, C., Lawrie, S., Lenroot, R.K., Lim, K.O., Lopez-Jaramillo, C., Lyall, A., Magnotta, V., Mandl, R.C.W., Mathalon, D.H., McCarley, R.W., McCarthy-Jones, S., McDonald, C., McEwen, S., McIntosh, A., Melicher, T., Mesholam-Gately, R.I., Michie, P.T., Mowry, B., Mueller, B.A., Newell, D.T., O'Donnell, P., Oertel-Knochel, V., Oestreich, L., Paciga, S.A., Pantelis, C., Pasternak, O., Pearlson, G., Pellicano, G.R., Pereira, A., Pineda Zapata, J., Piras, F., Potkin, S.G., Preda, A., Rasser, P.E., Roalf, D.R., Roiz, R., Roos, A., Rotenberg, D., Satterthwaite, T.D., Savadjiev, P., Schall, U., Scott, R.J., Seal, M.L., Seidman, L.J., Shannon Weickert, C., Whelan, C.D., Shenton, M.E., Kwon, J.S., Spalletta, G., Spaniel, F., Sprooten, E., Stablein, M., Stein, D.J., Sundram, S., Tan, Y., Tan, S., Tang, S., Temmingh, H.S., Westlye, L.T., Tonnesen, S., Tordesillas-Gutierrez, D., Doan, N.T., Vaidya, J., van Haren, N.E.M., Vargas, C.D., Vecchio, D., Velakoulis, D., Voineskos, A., Voyvodic, J.Q., Wang, Z., Wan, P., Wei, D., Weickert, T.W., Whalley, H., White, T., Whitford, T.J., Wojcik, J.D., Xiang, H., Xie, Z., Yamamori, H., Yang, F., Yao, N., Zhang, G., Zhao, J., van Erp, T.G.M., Turner, J., Thompson, P.M., Donohoe, G., 2017. Widespread white matter microstructural differences in schizophrenia across 4322 individuals: results from the ENIGMA Schizophrenia DTI Working Group. Mol. Psychiatry.
Keshavan, M.S., DeLisi, L.E., Seidman, L.J., 2011. Early and broadly defined psychosis risk mental states. Schizophr. Res. 126, 1–10.
Klauser, P., Zhou, J., Lim, J.K., Poh, J.S., Zheng, H., Tng, H.Y., Krishnan, R., Lee, J., Keefe, R.S., Adcock, R.A., Wood, S.J., Fornito, A., Chee, M.W., 2015. Lack of evidence for regional brain volume or cortical thickness abnormalities in youths at clinical high risk for psychosis: findings from the longitudinal youth at risk study. Schizophr. Bull.
Koch, K., Schultz, C.C., Wagner, G., Schachtzabel, C., Reichenbach, J.R., Sauer, H., Schlosser, R.G., 2013. Disrupted white matter connectivity is associated with reduced cortical thickness in the cingulate cortex in schizophrenia. Cortex 49, 722–729.
Koutsouleris, N., Patschurek-Kliche, K., Scheuerecker, J., Decker, P., Bottlender, R., Schmitt, G., Rujescu, D., Giegling, I., Gaser, C., Reiser, M., Moller, H.J., Meisenzahl, E.M., 2010. Neuroanatomical correlates of executive dysfunction in the at-risk mental state for psychosis. Schizophr. Res. 123, 160–174.
Krakauer, K., Ebdrup, B.H., Glenthoj, B.Y., Raghava, J.M., Nordholm, D., Randers, L., Rostrup, E., Nordentoft, M., 2017. Patterns of white matter microstructure in individuals at ultra-high-risk for psychosis: associations to level of functioning and clinical symptoms. Psychol. Med. 1–19.
Krakauer, K., Nordentoft, M., Glenthoj, B.Y., Raghava, J.M., Nordholm, D., Randers, L., Glenthoj, L.B., Ebdrup, B.H., Rostrup, E., 2018. White matter maturation during 12 months in individuals at ultra-high-risk for psychosis. Acta Psychiatr. Scand. 137, 65–78.
Kubota, M., Miyata, J., Sasamoto, A., Sugihara, G., Yoshida, H., Kawada, R., Fujimoto, S., Tanaka, Y., Sawamoto, N., Fukuyama, H., Takahashi, H., Murai, T., 2013. Thalamocortical disconnection in the orbitofrontal region associated with cortical thinning in schizophrenia. JAMA Psychiatry 70, 12–21.
Kumar, R., Nguyen, H.D., Macey, P.M., Woo, M.A., Harper, R.M., 2012. Regional brain axial and radial diffusivity changes during development. J. Neurosci. Res. 90, 346–355.
Kuperberg, G.R., Broome, M.R., McGuire, P.K., David, A.S., Eddy, M., Ozawa, F., Goff, D., West, W.C., Williams, S.C., van der Kouwe, A.J., Salat, D.H., Dale, A.M., Fischl, B., 2003. Regionally localized thinning of the cerebral cortex in schizophrenia. Arch. Gen. Psychiatry 60, 878–888.
Kwak, Y.B., Kim, M., Cho, K.I.K., Lee, J., Lee, T.Y., Kwon, J.S., 2019. Reduced cortical thickness in subjects at clinical high risk for psychosis and clinical attributes. Aust. N. Z. J. Psychiatry 53, 219–227.
Lee, T.Y., Hong, S.B., Shin, N.Y., Kwon, J.S., 2015. Social cognitive functioning in prodromal psychosis: a meta-analysis. Schizophr. Res. 164, 28–34.
Lei, W., Li, N., Deng, W., Li, M., Huang, C., Ma, X., Wang, Q., Guo, W., Li, Y., Jiang, L., Zhou, Y., Hu, X., Mary McAlonan, G., Li, T., 2015. White matter alterations in first episode treatment-naive patients with deficit schizophrenia: a combined VBM and DTI study. Sci. Rep. 5, 12994.
Lesh, T.A., Tanase, C., Geib, B.R., Niendam, T.A., Yoon, J.H., Minzenberg, M.J., Ragland, J.D., Solomon, M., Carter, C.S., 2015. A multimodal analysis of antipsychotic effects on brain structure and function in first-episode schizophrenia. JAMA Psychiatry 72, 226–234.
Lincoln, S.H., Norkett, E.M., Frost, K.H., Gonzalez-Heydrich, J., D'Angelo, E.J., 2017. A developmental perspective on social-cognition difficulties in youth at clinical high risk for psychosis. Harv. Rev. Psychiatry 25, 4–14.
Maas, D.A., Valles, A., Martens, G.J.M., 2017. Oxidative stress, prefrontal cortex hypomyelination and cognitive symptoms in schizophrenia. Transl. Psychiatry 7, e1171.
Mam-Lam-Fook, C., Danset-Alexandre, C., Pedron, L., Amado, I., Gaillard, R., Krebs, M.O., 2017. Neuropsychology of subjects with ultra-high risk (UHR) of psychosis: a critical analysis of the literature. Encephale 43, 241–253.
Mandl, R.C., Rais, M., van Baal, G.C., van Haren, N.E., Cahn, W., Kahn, R.S., Hulshoff Pol, H.E., 2013. Altered white matter connectivity in never-medicated patients with schizophrenia. Hum. Brain Mapp. 34, 2353–2365.
Marenco, S., Stein, J.L., Savostyanova, A.A., Sambataro, F., Tan, H.Y., Goldman, A.L., Verchinski, B.A., Barnett, A.S., Dickinson, D., Apud, J.A., Callicott, J.H., Meyer-Lindenberg, A., Weinberger, D.R., 2012. Investigation of anatomical thalamo-cortical connectivity and FMRI activation in schizophrenia. Neuropsychopharmacology 37, 499–507.
Middleton, F.A., Strick, P.L., 2001. A revised neuroanatomy of frontal-subcortical circuits. In: Lichter, D.G., Cummings, J.L. (Eds.), Frontal-Subcortical Circuits in Psychiatric and Neurological Disorders. The Guilford Press, New York London, pp. 44–58.
Mighdoll, M.I., Tao, R., Kleinman, J.E., Hyde, T.M., 2015. Myelin, myelin-related disorders, and psychosis. Schizophr. Res. 161, 85–93.
Miller, T.J., McGlashan, T.H., Woods, S.W., Stein, K., Driesen, N., Corcoran, C.M., Hoffman, R., Davidson, L., 1999. Symptom assessment in schizophrenic prodromal states. Psychiatr. Q. 70, 273–287.
Moser, D.A., Doucet, G.E., Lee, W.H., Rasgon, A., Krinsky, H., Leibu, E., Ing, A., Schumann, G., Rasgon, N., Frangou, S., 2018. Multivariate associations among behavioral, clinical, and multimodal imaging phenotypes in patients with psychosis. JAMA Psychiatry 75, 386–395.
Niu, J., Mei, F., Li, N., Wang, H., Li, X., Kong, J., Xiao, L., 2010. Haloperidol promotes proliferation but inhibits differentiation in rat oligodendrocyte progenitor cell cultures. Biochem. Cell Biol. 88, 611–620.
Olsen, K.A., Rosenbaum, B., 2006. Prospective investigations of the prodromal state of schizophrenia: assessment instruments. Acta Psychiatr. Scand. 113, 273–282.
Panizzon, M.S., Fennema-Notestine, C., Eyler, L.T., Jernigan, T.L., Prom-Wormley, E., Neale, M., Jacobson, K., Lyons, M.J., Grant, M.D., Franz, C.E., Xian, H., Tsuang, M., Fischl, B., Seidman, L., Dale, A., Kremen, W.S., 2009. Distinct genetic influences on cortical surface area and cortical thickness. Cereb. Cortex 19, 2728–2735.
Parnanzone, S., Serrone, D., Rossetti, M.C., D'Onofrio, S., Splendiani, A., Micelli, V., Rossi, A., Pacitti, F., 2017. Alterations of cerebral white matter structure in psychosis and their clinical correlations: a systematic review of diffusion tensor imaging studies. Riv. Psichiatr. 52, 49–66.
Pelletier-Baldelli, A., Bernard, J.A., Mittal, V.A., 2015. Intrinsic functional connectivity in salience and default mode networks and aberrant social processes in youth at ultra-high risk for psychosis. PLoS One 10, e0134936.
Peters, B.D., de Haan, L., Dekker, N., Blaas, J., Becker, H.E., Dingemans, P.M., Akkerman, E.M., Majoie, C.B., van Amelsvoort, T., den Heeten, G.J., Linszen, D.H., 2008. White matter fibertracking in first-episode schizophrenia, schizoaffective patients and subjects at ultra-high risk of psychosis. Neuropsychobiology 58, 19–28.
Peters, B.D., Dingemans, P.M., Dekker, N., Blaas, J., Akkerman, E., van Amelsvoort, T.A., Majoie, C.B., den Heeten, G.J., Linszen, D.H., de Haan, L., 2010. White matter connectivity and psychosis in ultra-high-risk subjects: a diffusion tensor fiber tracking study. Psychiatry Res. 181, 44–50.
Peters, B.D., Schmitz, N., Dingemans, P.M., van Amelsvoort, T.A., Linszen, D.H., de Haan, L., Majoie, C.B., den Heeten, G.J., 2009. Preliminary evidence for reduced frontal white matter integrity in subjects at ultra-high-risk for psychosis. Schizophr. Res. 111, 192–193.
Pollard, K.S., Dudoit, S., Laan, M.J., 2005. Multiple testing procedures: r multtest package and applications to genomics. In: Gentleman, R., Carey, V., Huber, W., Irizarry, R., Dudoit, S. (Eds.), Bioinformatics and Computational Biology Solutions Using R and Bioconductor. Springer Science+Business Media, New York, USA.
Reis Marques, T., Taylor, H., Chaddock, C., Dell'acqua, F., Handley, R., Reinders, A.A., Mondelli, V., Bonaccorso, S., Diforti, M., Simmons, A., David, A.S., Murray, R.M., Pariante, C.M., Kapur, S., Dazzan, P., 2014. White matter integrity as a predictor of response to treatment in first episode psychosis. Brain 137, 172–182.
Rietschel, L., Lambert, M., Karow, A., Zink, M., Muller, H., Heinz, A., de Millas, W., Janssen, B., Gaebel, W., Schneider, F., Naber, D., Juckel, G., Kruger-Ozgurdal, S., Wobrock, T., Wagner, M., Maier, W., Klosterkotter, J., Bechdolf, A., group, P.s., 2017. Clinical high risk for psychosis: gender differences in symptoms and social functioning. Early Intervention Psychiatry 11, 306–313.
Rigucci, S., Santi, G., Corigliano, V., Imola, A., Rossi-Espagnet, C., Mancinelli, I., De Pisa, E., Manfredi, G., Bozzao, A., Carducci, F., Girardi, P., Comparelli, A., 2016. White matter microstructure in ultra-high risk and first episode schizophrenia: a prospective study. Psychiatry Res 247, 42–48.
Rosas, H.D., Liu, A.K., Hersch, S., Glessner, M., Ferrante, R.J., Salat, D.H., van der Kouwe, A., Jenkins, B.G., Dale, A.M., Fischl, B., 2002. Regional and progressive thinning of the cortical ribbon in Huntington's disease. Neurology 58, 695–701.
Saito, J., Hori, M., Nemoto, T., Katagiri, N., Shimoji, K., Ito, S., Tsujino, N., Yamaguchi, T., Shiraga, N., Aoki, S., Mizuno, M., 2017. Longitudinal study examining abnormal white matter integrity using a tract-specific analysis in individuals with a high risk for psychosis. Psychiatry Clin. Neurosci. 71, 530–541.
Sarica, A., Cerasa, A., Vasta, R., Perrotta, P., Valentino, P., Mangone, G., Guzzi, P.H., Rocca, F., Nonnis, M., Cannataro, M., Quattrone, A., 2014. Tractography in amyotrophic lateral sclerosis using a novel probabilistic tool: a study with tract-based reconstruction compared to voxel-based approach. J. Neurosci. Methods 224, 79–87.
Sasamoto, A., Miyata, J., Kubota, M., Hirao, K., Kawada, R., Fujimoto, S., Tanaka, Y., Hazama, M., Sugihara, G., Sawamoto, N., Fukuyama, H., Takahashi, H., Murai, T., 2014. Global association between cortical thinning and white matter integrity reduction in schizophrenia. Schizophr. Bull. 40, 420–427.
Schmidt, A., Lenz, C., Smieskova, R., Harrisberger, F., Walter, A., Riecher-Rossler, A., Simon, A., Lang, U.E., McGuire, P., Fusar-Poli, P., Borgwardt, S.J., 2015. Brain diffusion changes in emerging psychosis and the impact of state-dependent psychopathology. Neurosignals 23, 71–83.
Schmidt, A., Smieskova, R., Simon, A., Allen, P., Fusar-Poli, P., McGuire, P.K., Bendfeldt, K., Aston, J., Lang, U.E., Walter, M., Radue, E.W., Riecher-Rossler, A., Borgwardt, S.J., 2014. Abnormal effective connectivity and psychopathological symptoms in the psychosis high-risk state. J. Psychiatry Neurosci. 39, 239–248.

Serpa, M.H., Doshi, J., Erus, G., Chaim-Avancini, T.M., Cavallet, M., van de Bilt, M.T., Sallet, P.C., Gattaz, W.F., Davatzikos, C., Busatto, G.F., Zanetti, M.V., 2017. State-dependent microstructural white matter changes in drug-naive patients with first-episode psychosis. Psychol. Med. 47, 2613–2627.
Sherman, S.M., 2016. Thalamus plays a central role in ongoing cortical functioning. Nat. Neurosci. 19, 533–541.
Shim, G., Oh, J.S., Jung, W.H., Jang, J.H., Choi, C.H., Kim, E., Park, H.Y., Choi, J.S., Jung, M.H., Kwon, J.S., 2010. Altered resting-state connectivity in subjects at ultra-high risk for psychosis: an fMRI study. Behav Brain Funct. 6, 58.
Smith, S.M., Jenkinson, M., Johansen-Berg, H., Rueckert, D., Nichols, T.E., Mackay, C.E., Watkins, K.E., Ciccarelli, O., Cader, M.Z., Matthews, P.M., Behrens, T.E., 2006. Tract-based spatial statistics: voxelwise analysis of multi-subject diffusion data. Neuroimage 31, 1487–1505.
Song, S.K., Yoshino, J., Le, T.Q., Lin, S.J., Sun, S.W., Cross, A.H., Armstrong, R.C., 2005. Demyelination increases radial diffusivity in corpus callosum of mouse brain. Neuroimage 26, 132–140.
Song, X., Quan, M., Lv, L., Li, X., Pang, L., Kennedy, D., Hodge, S., Harrington, A., Ziedonis, D., Fan, X., 2015. Decreased cortical thickness in drug naive first episode schizophrenia: in relation to serum levels of BDNF. J. Psychiatr. Res. 60, 22–28.
Squarcina, L., Bellani, M., Rossetti, M.G., Perlini, C., Delvecchio, G., Dusi, N., Barillari, M., Ruggeri, M., Altamura, C.A., Bertoldo, A., Brambilla, P., 2017. Similar white matter changes in schizophrenia and bipolar disorder: a tract-based spatial statistics study. PLoS One 12, e0178089.
Sui, J., Pearlson, G.D., Du, Y., Yu, Q., Jones, T.R., Chen, J., Jiang, T., Bustillo, J., Calhoun, V.D., 2015. In search of multimodal neuroimaging biomarkers of cognitive deficits in schizophrenia. Biol. Psychiatry 78, 794–804.
Sun, H., Lui, S., Yao, L., Deng, W., Xiao, Y., Zhang, W., Huang, X., Hu, J., Bi, F., Li, T., Sweeney, J.A., Gong, Q., 2015. Two patterns of white matter abnormalities in medication-naive patients with first-episode schizophrenia revealed by diffusion tensor imaging and cluster analysis. JAMA Psychiatry.
Sun, S.W., Liang, H.F., Le, T.Q., Armstrong, R.C., Cross, A.H., Song, S.K., 2006. Differential sensitivity of in vivo and ex vivo diffusion tensor imaging to evolving optic nerve injury in mice with retinal ischemia. Neuroimage 32, 1195–1204.
Szeszko, P.R., Robinson, D.G., Ikuta, T., Peters, B.D., Gallego, J.A., Kane, J., Malhotra, A.K., 2014. White matter changes associated with antipsychotic treatment in first-episode psychosis. Neuropsychopharmacology 39, 1324–1331.
Takayanagi, Y., Kulason, S., Sasabayashi, D., Takahashi, T., Katagiri, N., Sakuma, A., Obara, C., Nakamura, M., Kido, M., Furuichi, A., Nishikawa, Y., Noguchi, K., Matsumoto, K., Mizuno, M., Ratnanather, J.T., Suzuki, M., 2017. Reduced thickness of the anterior cingulate cortex in individuals with an at-risk mental state who later develop psychosis. Schizophr. Bull. 43, 907–913.
Tamnes, C.K., Ostby, Y., Fjell, A.M., Westlye, L.T., Due-Tonnessen, P., Walhovd, K.B., 2010. Brain maturation in adolescence and young adulthood: regional age-related changes in cortical thickness and white matter volume and microstructure. Cereb. Cortex 20, 534–548.
Tognin, S., Riecher-Rossler, A., Meisenzahl, E.M., Wood, S.J., Hutton, C., Borgwardt, S.J., Koutsouleris, N., Yung, A.R., Allen, P., Phillips, L.J., McGorry, P.D., Valli, I., Velakoulis, D., Nelson, B., Woolley, J., Pantelis, C., McGuire, P., Mechelli, A., 2014. Reduced parahippocampal cortical thickness in subjects at ultra-high risk for psychosis. Psychol. Med. 44, 489–498.
van Erp, T.G.M., Walton, E., Hibar, D.P., Schmaal, L., Jiang, W., Glahn, D.C., Pearlson, G.D., Yao, N., Fukunaga, M., Hashimoto, R., Okada, N., Yamamori, H., Bustillo, J.R., Clark, V.P., Agartz, I., Mueller, B.A., Cahn, W., de Zwarte, S.M.C., Hulshoff Pol, H.E., Kahn, R.S., Ophoff, R.A., van Haren, N.E.M., Andreassen, O.A., Dale, A.M., Doan, N.T., Gurholt, T.P., Hartberg, C.B., Haukvik, U.K., Jorgensen, K.N., Lagerberg, T.V., Melle, I., Westlye, L.T., Gruber, O., Kraemer, B., Richter, A., Zilles, D., Calhoun, V.D., Crespo-Facorro, B., Roiz-Santianez, R., Tordesillas-Gutierrez, D., Loughland, C., Carr, V.J., Catts, S., Cropley, V.L., Fullerton, J.M., Green, M.J., Henskens, F.A., Jablensky, A., Lenroot, R.K., Mowry, B.J., Michie, P.T., Pantelis, C., Quide, Y., Schall, U., Scott, R.J., Cairns, M.J., Seal, M., Tooney, P.A., Rasser, P.E., Cooper, G., Shannon Weickert, C., Weickert, T.W., Morris, D.W., Hong, E., Kochunov, P., Beard, L.M., Gur, R.E., Gur, R.C., Satterthwaite, T.D., Wolf, D.H., Belger, A., Brown, G.G., Ford, J.M., Macciardi, F., Mathalon, D.H., O'Leary, D.S., Potkin, S.G., Preda, A., Voyvodic, J., Lim, K.O., McEwen, S., Yang, F., Tan, Y., Tan, S., Wang, Z., Fan, F., Chen, J., Xiang, H., Tang, S., Guo, H., Wan, P., Wei, D., Bockholt, H.J., Ehrlich, S., Wolthusen, R.P.F., King, M.D., Shoemaker, J.M., Sponheim, S.R., De Haan, L., Koenders, L., Machielsen, M.W., van Amelsvoort, T., Veltman, D.J., Assogna, F., Banaj, N., de Rossi, P., Iorio, M., Piras, F., Spalletta, G., McKenna, P.J., Pomarol-Clotet, E., Salvador, R., Corvin, A., Donohoe, G., Kelly, S., Whelan, C.D., Dickie, E.W., Rotenberg, D., Voineskos, A.N., Ciufolini, S., Radua, J., Dazzan, P., Murray, R., Reis Marques, T., Simmons, A., Borgwardt, S., Egloff, L., Harrisberger, F., Riecher-Rossler, A., Smieskova, R., Alpert, K.I., Wang, L., Jonsson, E.G., Koops, S., Sommer, I.E.C., Bertolino, A., Bonvino, A., Di Giorgio, A., Neilson, E., Mayer, A.R., Stephen, J.M., Kwon, J.S., Yun, J.Y., Cannon, D.M., McDonald, C., Lebedeva, I., Tomyshev, A.S., Akhadov, T., Kaleda, V., Fatouros-Bergman, H., Flyckt, L., Karolinska Schizophrenia, P., Busatto, G.F., Rosa, P.G.P., Serpa, M.H., Zanetti, M.V., Hoschl, C., Skoch, A., Spaniel, F., Tomecek, D., Hagenaars, S.P., McIntosh, A.M., Whalley, H.C., Lawrie, S.M., Knochel, C., Oertel-Knochel, V., Stablein, M., Howells, F.M., Stein, D.J., Temmingh, H.S., Uhlmann, A., Lopez-Jaramillo, C., Dima, D., McMahon, A., Faskowitz, J.I., Gutman, B.A., Jahanshad, N., Thompson, P.M., Turner, J.A., 2018. Cortical brain abnormalities in 4474 individuals with schizophrenia and 5098 control subjects via the enhancing neuro imaging genetics through meta analysis (ENIGMA) consortium. Biol. Psychiatry 84, 644–654.
Van Essen, D.C., 1997. A tension-based theory of morphogenesis and compact wiring in the central nervous system. Nature 385, 313–318.
van Lutterveld, R., van den Heuvel, M.P., Diederen, K.M., de Weijer, A.D., Begemann, M.J., Brouwer, R.M., Daalman, K., Blom, J.D., Kahn, R.S., Sommer, I.E., 2014. Cortical thickness in individuals with non-clinical and clinical psychotic symptoms. Brain 137, 2664–2669.
Vita, A., De Peri, L., Deste, G., Barlati, S., Sacchetti, E., 2015. The effect of antipsychotic treatment on cortical gray matter changes in schizophrenia: does the class matter? A meta-analysis and meta-regression of longitudinal magnetic resonance imaging studies. Biol. Psychiatry 78, 403–412.
von Hohenberg, C.C., Pasternak, O., Kubicki, M., Ballinger, T., Vu, M.A., Swisher, T., Green, K., Giwerc, M., Dahlben, B., Goldstein, J.M., Woo, T.U., Petryshen, T.L., Mesholam-Gately, R.I., Woodberry, K.A., Thermenos, H.W., Mulert, C., McCarley, R.W., Seidman, L.J., Shenton, M.E., 2014. White matter microstructure in individuals at clinical high risk of psychosis: a whole-brain diffusion tensor imaging study. Schizophr. Bull. 40, 895–903.
Walton, E., Hibar, D.P., van Erp, T.G.M., Potkin, S.G., Roiz-Santianez, R., Crespo-Facorro, B., Suarez-Pinilla, P., van Haren, N.E.M., de Zwarte, S.M.C., Kahn, R.S., Cahn, W., Doan, N.T., Jorgensen, K.N., Gurholt, T.P., Agartz, I., Andreassen, O.A., Westlye, L.T., Melle, I., Berg, A.O., Morch-Johnsen, L., Faerden, A., Flyckt, L., Fatouros-Bergman, H., Karolinska Schizophrenia Project, C., Jonsson, E.G., Hashimoto, R., Yamamori, H., Fukunaga, M., Jahanshad, N., De Rossi, P., Piras, F., Banaj, N., Spalletta, G., Gur, R.E., Gur, R.C., Wolf, D.H., Satterthwaite, T.D., Beard, L.M., Sommer, I.E., Koops, S., Gruber, O., Richter, A., Kramer, B., Kelly, S., Donohoe, G., McDonald, C., Cannon, D.M., Corvin, A., Gill, M., Di Giorgio, A., Bertolino, A., Lawrie, S., Nickson, T., Whalley, H.C., Neilson, E., Calhoun, V.D., Thompson, P.M., Turner, J.A., Ehrlich, S., 2018. Prefrontal cortical thinning links to negative symptoms in schizophrenia via the ENIGMA consortium. Psychol. Med. 48, 82–94.
Wang, C., Ji, F., Hong, Z., Poh, J.S., Krishnan, R., Lee, J., Rekhi, G., Keefe, R.S., Adcock, R.A., Wood, S.J., Fornito, A., Pasternak, O., Chee, M.W., Zhou, J., 2016a. Disrupted salience network functional connectivity and white-matter microstructure in persons at risk for psychosis: findings from the LYRIKS study. Psychol. Med. 46, 2771–2783.
Wang, H., Guo, W., Liu, F., Wang, G., Lyu, H., Wu, R., Chen, J., Wang, S., Li, L., Zhao, J., 2016b. Patients with first-episode, drug-naive schizophrenia and subjects at ultra-high risk of psychosis shared increased cerebellar-default mode network connectivity at rest. Sci. Rep. 6, 26124.
Wang, Q., Cheung, C., Deng, W., Li, M., Huang, C., Ma, X., Wang, Y., Jiang, L., Sham, P.C., Collier, D.A., Gong, Q., Chua, S.E., McAlonan, G.M., Li, T., 2013. White-matter microstructure in previously drug-naive patients with schizophrenia after 6 weeks of treatment. Psychol. Med. 43, 2301–2309.
Woods, S.W., Miller, T.J., McGlashan, T.H., 2001. The "prodromal" patient: both symptomatic and at-risk. CNS Spectrums 6, 223–232.
Wotruba, D., Michels, L., Buechler, R., Metzler, S., Theodoridou, A., Gerstenberg, M., Walitza, S., Kollias, S., Rossler, W., Heekeren, K., 2014. Aberrant coupling within and across the default mode, task-positive, and salience network in subjects at risk for psychosis. Schizophr. Bull. 40, 1095–1104.
Xiao, L., Xu, H., Zhang, Y., Wei, Z., He, J., Jiang, W., Li, X., Dyck, L.E., Devon, R.M., Deng, Y., Li, X.M., 2008. Quetiapine facilitates oligodendrocyte development and prevents mice from myelin breakdown and behavioral changes. Mol. Psychiatry 13, 697–708.
Xiao, Y., Lui, S., Deng, W., Yao, L., Zhang, W., Li, S., Wu, M., Xie, T., He, Y., Huang, X., Hu, J., Bi, F., Li, T., Gong, Q., 2015. Altered cortical thickness related to clinical severity but not the untreated disease duration in schizophrenia. Schizophr. Bull. 41, 201–210.
Yendiki, A., Panneck, P., Srinivasan, P., Stevens, A., Zollei, L., Augustinack, J., Wang, R., Salat, D., Ehrlich, S., Behrens, T., Jbabdi, S., Gollub, R., Fischl, B., 2011. Automated probabilistic reconstruction of white-matter pathways in health and disease using an atlas of the underlying anatomy. Front. Neuroinform. 5, 23.
Yeo, B.T., Krienen, F.M., Sepulcre, J., Sabuncu, M.R., Lashkari, D., Hollinshead, M., Roffman, J.L., Smoller, J.W., Zollei, L., Polimeni, J.R., Fischl, B., Liu, H., Buckner, R.L., 2011. The organization of the human cerebral cortex estimated by intrinsic functional connectivity. J. Neurophysiol. 106, 1125–1165.
Zeng, B., Ardekani, B.A., Tang, Y., Zhang, T., Zhao, S., Cui, H., Fan, X., Zhuo, K., Li, C., Xu, Y., Goff, D.C., Wang, J., 2016. Abnormal white matter microstructure in drug-naive first episode schizophrenia patients before and after eight weeks of antipsychotic treatment. Schizophr. Res. 172, 1–8.
Ziermans, T.B., Schothorst, P.F., Schnack, H.G., Koolschijn, P.C., Kahn, R.S., van Engeland, H., Durston, S., 2012. Progressive structural brain changes during development of psychosis. Schizophr. Bull. 38, 519–530.